

RESEARCH ARTICLE

 OPEN ACCESS

Received: 25-01-2022

Accepted: 18-04-2022

Published: 25-05-2022

Citation: Kumar BMH, Vaibhav AM, Srikanth PC (2022) Si/SiO₂ Based Nano-cavity Biosensor for Detection of Anemia, HIV and Cholesterol Using Refractive Index of Blood Sample. Indian Journal of Science and Technology 15(18): 899-907. <https://doi.org/10.17485/IJST/v15i18.186>

* Corresponding author.

hemanthkrn86@gmail.com

Funding: None

Competing Interests: None

Copyright: © 2022 Kumar et al. This is an open access article distributed under the terms of the [Creative Commons Attribution License](https://creativecommons.org/licenses/by/4.0/), which permits unrestricted use, distribution, and reproduction in any medium, provided the original author and source are credited.

Published By Indian Society for Education and Environment ([iSee](https://www.indjst.org/))

ISSN

Print: 0974-6846

Electronic: 0974-5645

Si/SiO₂ Based Nano-cavity Biosensor for Detection of Anemia, HIV and Cholesterol Using Refractive Index of Blood Sample

B M Hemanth Kumar^{1*}, AM Vaibhav², P C Srikanth³¹ Research Scholar, Dayananda Sagar University, Bengaluru, India² Dept. of E & C Engineering, Dayananda Sagar University, Bengaluru, India³ Dept. of E & C Engineering, Malnad College of Engineering, Hassan, India

Abstract

Objectives: To model photonic multipurpose biosensor for detection of sickle cell anemia, HIV and cholesterol by its refractive index using FDTD method.

Methods: The proposed multipurpose photonic biosensor has 12μm X 08μm dimension designed using Lumerical software. Blood sample is deposited inside the hole cavity of sensor and gaussian light source of 1.5 – 1.6 μm wavelength is injected inside the waveguide, based on the refractive index of disease sample to the normal sample there will be shift in the wavelength. FDTD method is used for simulating the PhC silicon sensor. When body gets infected there will be changes in physical as well as biological composition results in disparity of refractive index of biological component. Resonating frequency will be displayed in DFT monitor at the output waveguide. **Findings:** Based on the RI value the resonating wavelength shifts inside the bandgap of frequency spectrum. By comparing with the normal value there is shift in wavelength of 03nm, 08nm and 22nm for anemia, HIV and Cholesterol respectively. Biosensor has Quality factor of 257, tolerance factor 3% and the sensitivity obtained for change in RI of the sample is 225 nm/RIU. **Novelty:** The proposed biosensor functions as multipurpose detector and design is compatible in detecting anemia, HIV and Cholesterol in photonics platform. Novel signature analysis is performed by using polar plot for distinguishing the disease in early stage.

Keywords: Photonic Crystal; Refractive index; Red blood corpuscles; Human immunodeficiency virus; Finite difference time domain; Photonic bandgap

1 Introduction

Photonics is advanced and emerging technology in medical and biological applications. Photonic crystals are artificial periodic dielectric structures arranged alternatively with different refractive index creates band gap that forbids propagation of a certain frequency range of light, this enables photonic crystals to control light and produce effects that are impossible with conventional optics⁽¹⁾. In photonic biosensing environment, the volume of detecting sample is in terms of micro or nano scale and the

indicating output frequency spectrum is highly dependent on refractive index. Photonic sensor is highly desirable compared to electronic sensor due to very low development cost, highly sensitive to change in parameters, label-free and user friendly.

Photonic biosensors are used to detect various cancer cells in humans and it is used to identify different biological components. The photonic biosensor is sensitive to change in physical and chemical composition of the blood sample affected by anemia, HIV and cholesterol. Sickle cell anaemia is a type of blood disorder results in less oxygen carrying capacity in the RBC throughout the body blood vessels. HIV infected persons has very low WBC count in blood causes reduction in disease fighting capability. Heavy bad cholesterol in blood plasma will combine with materials in the blood to form plaque that will get stuck into the inner walls of the arteries. This will cause atherosclerosis leads to heart artery disease.

In⁽²⁾ 2D PhC biosensor is designed for detecting malaria using RBC sample. The structure is made up of elliptical silicon nitride rods with ring resonator and FDTD method is used for simulation. In this structure placing sample is very difficult as it uses rods in air configuration and maximum Q-factor obtained is only 172. In⁽³⁾ 1D photonic crystal biosensor is proposed to detect blood plasma and cancer cells. Bandgap is created using alternating material of SiO₂ and TiO₂ layer, achieves sensitivity of 71.25 nm/RIU for sensor thickness of 100nm and sensitivity is increased by changing the sensor thickness to 300nm. Here sensitivity is less for detecting cancer cells. In⁽⁴⁾ photonic crystal biosensor sensor has been modelled in 1D to detect of poliovirus (PV) in water. To investigate the transmission spectrum, it uses transfer matrix method and sensor work at 260nm wavelength. Compare to FDTD method; transfer matrix method gives less sensitivity and its efficiency is moderate. In⁽⁵⁾ for detecting different types of skin cancer a 1D photonic crystal biosensor is designed. It uses gradient index lens in the middle of structure and two fluid layers around the lens. In this method placing of lens is really a challenging task since size of photonic sensor is very small in size. Detection of anemia is done using complete blood count, peripheral blood smear method, Solubility Sickling Test, Image processing technique etc.⁽⁶⁾ HIV detection is done by rapid antigen testing, molecular method etc. but these techniques have more chances of false results and diagnosis time is large⁽⁷⁾. For detecting cholesterol level various analytical methods are used; liquid chromatography, molecular imprinting polymer (MIP) technology, fluorescence, chemiluminescence, and electrochemistry⁽⁸⁾. These detection methods are complex procedure, require point of care testing environment, requires more processing time and more chances of false report. Photonic biosensor is label-free detection and its detection method is based on bio-sample refractive index depends on chemical, physical and mechanical composition. The proposed model is unaccustomed by its compatibility in detection of anemia, HIV and cholesterol. Pre-processing of sample is not required; in the proposed model sensitivity is improved for detecting multi-diseases and it is easily distinguishable using novel signature analysis by comparing with normal polar plot in terms of radiation angle.

2 Photonics

A PBG crystal is a compound structure that will manipulate light beams as semiconductors control electrons. Semiconductor will not support electrons in the electronic band gap region. Similarly, a photonic crystal structure will not allow photons in the photonic band gap region. These crystals allow or blocks the light based on parameters of crystal and light wavelength. The bandgap of PhC is a function of wavelength, RI of the material, the periodic array material RI and the lattice constant kept between the holes in crystal structure⁽⁹⁾. Given by Bragg's law equation:

$$2d \sin \theta = n\lambda \quad (1)$$

Where 'd' is distance between holes or rods, 'θ' is the incidence angle with respect to normal, 'λ' is the light wavelength. Light entering the dielectric structure will undergo reflection and refraction at the interfaces. The regular or complex pattern of overlapping waves will lead to cancellation of a certain band of frequencies in all possible directions leading to prevention of propagation of certain band of light in the crystal. The dielectric photonic band structure can be altered by filling some holes or introducing defects in the crystal structure.

The Photonic bandgap is also a function of sensor holes radius and the incident light frequency from laser source. Photonic crystal is mainly grouped on the material arrangement such as 1-D crystal structure, 2-D crystal structure and 3-D structures. These classifications are based on structural arrangement. 3D structures are more accurate structures but its complexity in fabrication leads to error of model. In the proposed work 2-dimensional structure is used, because 2D crystal has better light confinement inside the sensor and fabrication of 2D structures is simple. To introduce light modes, defects are introduced in the array of holes in the model by taking off certain number of holes and tuning certain holes size⁽¹⁰⁾. In photonic crystals PBG is formed, by introducing defects it changes propagation properties results in some frequency modes inside the PBG. This interesting property of PhC is used for the sensor design.

Light propagation in photonic crystals is related by the Maxwell's equation of electromagnetic waves.

$$\nabla \cdot B = 0 \quad (2)$$

$$\nabla \times E + \frac{\partial B}{\partial t} = 0 \quad (3)$$

$$\nabla \cdot D = \rho \quad (4)$$

$$\nabla \times H - \frac{\partial D}{\partial t} = J \quad (5)$$

Where 'E' relates electric field and 'H' is displacement magnetic field and 'B' is induction magnetic field, 'ρ' is free charge and 'J' is density of current in structure.

The time differing EM fields apply with Maxwell's equations are as follows

$$\nabla \cdot H(r,t) = 0 \quad (6)$$

$$\nabla \times E(r,t) = -\mu(r) \frac{\partial H(r,t)}{\partial t} \quad (7)$$

$$\nabla \times H(r,t) = \sigma(r)E(r,t) + \epsilon(r) \frac{\partial E(r,t)}{\partial t} \quad (8)$$

$$\nabla \cdot E(r,t) = \frac{\rho(r,t)}{\epsilon(r)} \quad (9)$$

Where $E(r,t)$ and $H(r,t)$ are time varying Electric and Magnetic fields in the structure and $\epsilon(r)$, $\mu(r)$ are permittivity and permeability of material, $\sigma(r)$ conductivity of the medium.

In optical waveguide the propagation of light is carted out by solving the below equation:

$$\nabla^2 \epsilon(x_0 y_2 z) + K^2 \epsilon(x_0 y_2 z) = 0 \quad (10)$$

Where $k = k_0 n(x,y,z)$ with $k_0 = 2\pi/\lambda$, $n(x,y,z)$ gives RI of the given medium and λ is the wavelength of the light. The FDTD method is used for the analysis of wave propagation in sensor devices and it is generally used to analyse electromagnetic phenomena at radio and microwave frequencies. In the FDTD, the wave equation is divided in both space and time, the propagation of an input electric field is carried out progressively and PML boundary condition is set for the absorption of the waves at the boundary. In this method cells are formed by differentiating design space into small areas. On the surfaces of every cell, there are relegated focuses. Inside a limited volume of space, the electromagnetic field is tested continuously, fields are examined at every regular discrete space grid and at discrete focuses in time. FDTD method allows finding the field distribution by solving the system of Maxwell's equations upon the discrete mesh. The solution is based on Permittivity distribution function intern determines radiation propagation conditions, initial conditions such as the wavelength, amplitude and initial phase. Boundary conditions determine the radiation behavior at the boundary of the computation region.

3 Biosensor Design

For the multipurpose biosensor design two-layer model is used, top layer is sensing layer with silicon material and the bottom layer is SiO₂ with refractive index of 1.48 gives physical strength for the sensor⁽¹¹⁾. In top layer first etching is done and holes array is created. Line defect is created by removing centre line holes, but in the defect line 8 holes are not removed for tuning the sensitivity of the sensor. The centre four holes are 100 nm and the bigger holes are 160 nm. Thickness of the sensor is 30 nm, inside this hole cavity blood sample is filled to diagnose the diseases. The length and breadth of the sensor is 12 μm X 08 μm. To the input end of line defect a gaussian light source having wavelength of 1.5 μm to 1.6 μm is placed to the input interfering end of the waveguide. To record the readings, power and frequency monitor is kept at the output end of waveguide, smooth curve is plotted by setting simulation points to 500. Perfectly matched layer (PML) is set to the boundary condition to absorb the out radiated energy from the sensor. To avoid the temperature or any external factor variation, a mesh is placed around

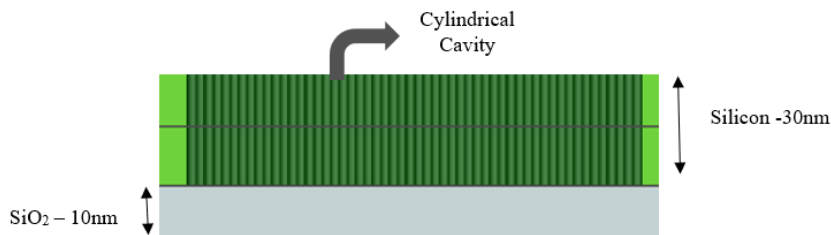


Fig 1. Front view of the model

the boundary of the structure⁽¹²⁾. The structure is set to 2D FDTD, 500 simulation plots are covering the boundary in X and Y direction of the model. The designing of the sensor and the simulation is done by Lumerical software.

Figure 1 depicts sensor front image in X-Z plane, lower or bottom layer is composed using silicon dioxide material and the upper layer of design performs sensing of diseases.

Design parameters of the sensor:

- Lattice structure- Hexagonal
- Radius of the sensor holes – 130nm
- Lattice constant - 420nm
- Base (SiO₂) refractive index – 1.48
- Sensor (Si) Refractive index – 3.45
- Normal blood sample RI – 1.35
- Sickle cell anemia sample RI – 1.38
- HIV infected sample RI – 1.42
- Blood sample having high cholesterol RI – 1.52
- Light source width - 1.5 to 1.6 μm

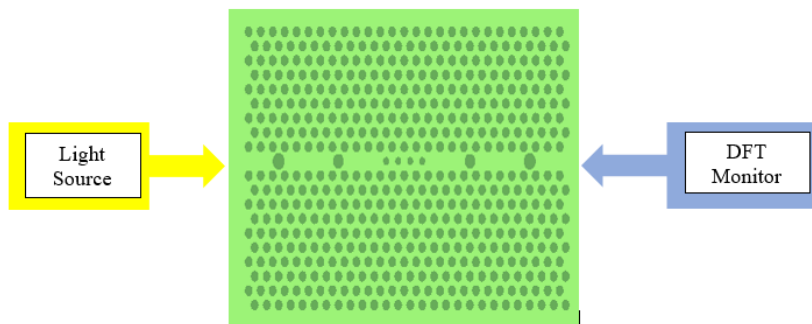


Fig 2. Model top view

Figure 2 represents proposed 2-D model with top X-Y plane. Waveguide is implanted by taking off some of holes from light input end to monitor output end results in line defect. All the holes radius of the array is maintained constant and some of hole's radius in line waveguide is changed to increase the quality factor of sensor. Blood samples are introduced inside the cavity of the crystal slab. The simulation is done in the air surrounding medium; hence background index is kept to one, it is the RI value of air.

4 Simulation Results

This section consists of 2D-FDTD simulation results and analysis of the transmission spectrum. For simulation disinfected blood refractive index of 1.35 assigned to the holes filled with sample. At the input end, from laser source a light beam is passed to the input port of waveguide with wavelength 1.5 - 1.6 μm. For every disease analysis two iteration is done, first all holes are filled with normal blood and its transmission plot is noted using DFT monitor. In the next iteration holes of sensor are capped with the refractive index of the corresponding diseases such as 1.38 for sickle cell anaemia, 1.42 for HIV and 1.52 for high

density cholesterol. The obtained transmission spectrum is compared with normal spectrum. Sickle cell anaemia, cholesterol and HIV are having different refractive index results in different shift in wavelength curve of the output spectrum. The PBG of the crystal mainly depends on the lattice structure, material used, lattice constant and refractive index⁽¹³⁾. The photonic crystal biosensor without introducing line defect has bandgap range from 1450 to 1925nm wavelength.

Detection methodology of biosensor:

- Patient blood sample is collected.
- Biosensor holes is filled with the collected sample.
- Pass laser light inside the sensor waveguide.
- Analyse the output curve and note monitor readings.
- Compare the obtained reading with normal signature reading.
- If there is shift in the resonant frequency of the curve from the normal signature, then the person is infected by the disease.
- If the output resonant frequency is not showing any shift, then the person is normal.

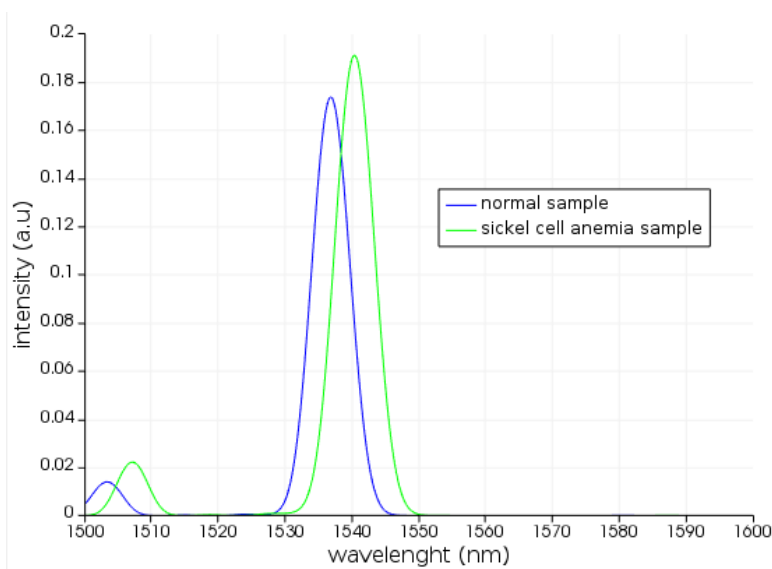


Fig 3. Transmission spectra of sickle cell anaemia sample

In Figure 3 shift in the curve is shown for normal blood sample and the RBC infected sickle cell anemia sample. Both the wavelength shift and intensity shift are calculated⁽¹⁴⁾, these reading are used to calculate the quality factor and the sensitivity of the biosensor. In the same manner the execution is done for the cholesterol and the HIV sample and its Q-factor and corresponding sensitivity is noted. For anemia, wavelength is shifted by 03nm and has intensity variation of 0.02 a.u in the transmission curve. Figure 6 shows normal blood sample curve comparison with a RBC infected sickle cell anaemia blood sample, HIV infected blood sample and high cholesterol blood sample.

Table 1. Shift in resonant wavelength and Intensity of disease samples

Type of cell	Resonant λ	λ shift	Intensity	Intensity shift
Normal sample	1537 nm	-	0.22	-
Sickle cell anemia sample	1540 nm	03 nm	0.24	0.02 a.u
HIV infected sample	1545 nm	08 nm	0.27	0.05 a.u
Blood sample having high cholesterol	1559 nm	22 nm	0.26	0.04 a.u

Table 1 gives the amount of wavelength shift and intensity changes in both the iterations for sickle cell anaemia, HIV and Cholesterol. In the table, diseases are having different wavelength shift and change in the intensity due to the difference in refractive index. This factor makes this sensor to use as multipurpose sensor. Shift in the resonant wavelength and intensity is purely dependent on the refractive of the sample taken for analysis. The RI value of sickle cell anaemia is 1.38, compared to

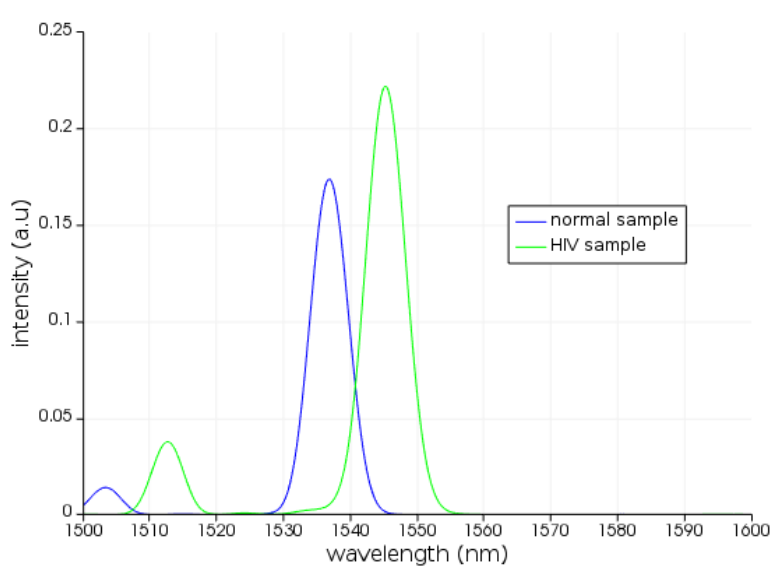


Fig 4. Transmission spectra of HIV infected sample

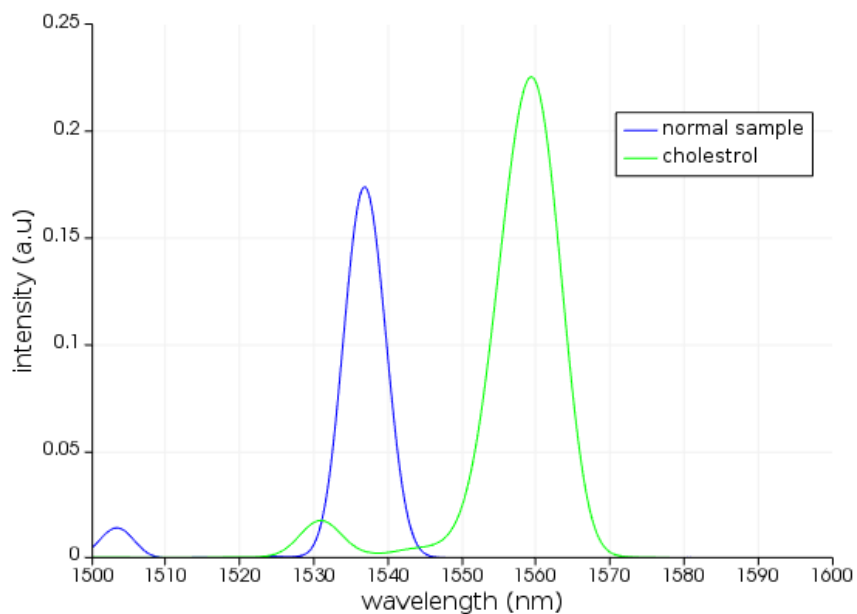


Fig 5. Transmission spectra of high-density cholesterol blood sample

normal sample it is 0.03 units high, it is having resonant shift of 03nm. RI value of HIV sample is 1.42 and Cholesterol sample RI value is 1.52, the obtained wavelength shift is 08nm and 22nm respectively.

The multipurpose biosensor efficiency is determined by quality factor and obtained sensitivity of the model. Q-factor is the ratio obtained between resonant wavelength and difference obtained at the wavelength at full width of the resonant mode at half power⁽¹⁵⁾.

$$Q = \frac{\lambda_r}{FWHM}$$

Where ' λ_r ' maximum peak resonating wavelength of the curve and FWHM is full width half maximum wavelength.

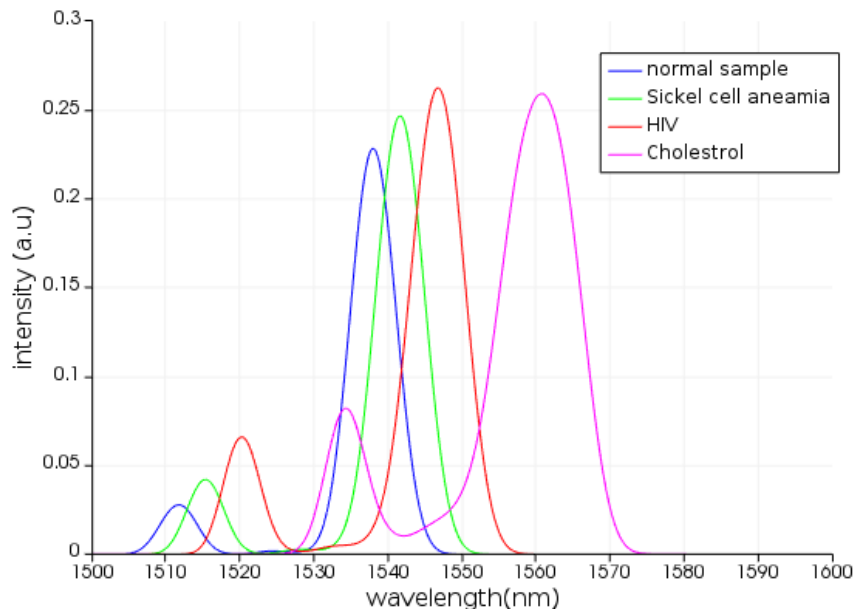


Fig 6. Transmission spectra of multipurpose sensor.

Sensitivity is given as difference in the resonating mode wavelength ($\Delta\lambda$) to the corresponding change in the RI of the sample (Δn)⁽¹⁶⁾. Sensitivity is critical parameters in detection of diseases, The obtained sensitivity for this model is 225nm/RIU

$$s = \frac{\Delta\lambda}{\Delta n}$$

In the line defect centre four holes radius is varied to achieve maximum quality factor of the sensor. For holes size 100nm achieved FWHM is 6 and obtained maximum quality factor of 257. Quality factor and sensitivity is a function of hole size and lattice constant. Samples placed inside the holes will impact the resonating wavelength.

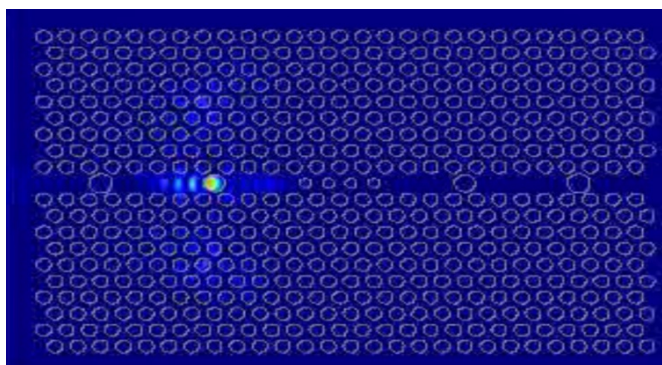


Fig 7. Electric field wave propagation in the crystal.

Figure 7 show the electric field propagation inside the sensor waveguide when the gaussian light sensor is passed. In figure it can be seen that the light propagates in the waveguide through the defects. When light propagates complete light is not propagated, there is some amount of loss due to the destructive interference⁽¹⁷⁾.

Figure 8 shows the polar plot used for the signature analysis of diseases. It gives signature mark in disease analysis; it exhibits the intensity at different angle for the different diseases. The normal plot will be compared with the infected plot in terms of cross leaf angle. For normal sample cross leaf angle is 320°, anemia - 235°, HIV - 305° and for cholesterol - 30°. Polar plot is sensitive to RI of sample, based on this the leaf angle varies in the signature.

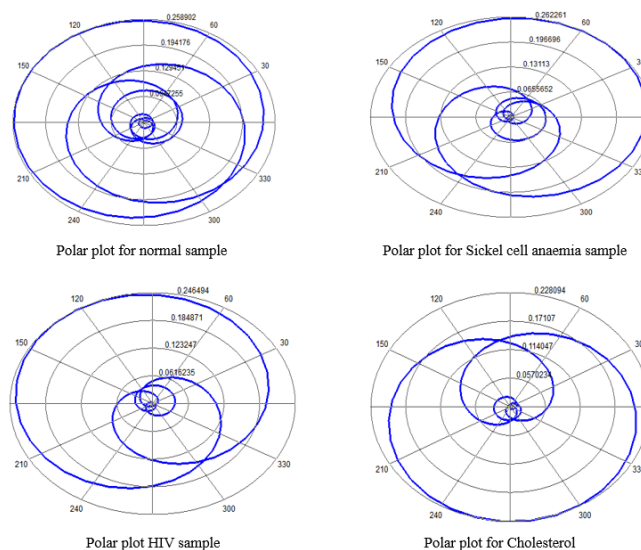


Fig 8. Signature analysis of diseases using Polar plot

5 Conclusion

There are numerous methods to detect anemia, HIV and cholesterol level in humans, but in conventional methods there are limitations and drawbacks in terms of false reports, complexity and diagnosis time. To evade this a multipurpose nano-biosensor is designed in the photonics platform and FDTD method is used for simulating the electromagnetic wave propagation. The photonic sensor uses light as source, it is label-free and uses refractive index of bio-sample, hence pre-processing of the sample is not required. The run time of the model is less than 2 minutes and it can be used as rapid testing model. The sensor is multifunctional, this single design is compatible in detecting three diseases hence design cost is reduced. The sensor is more efficient having sensitivity of 225 nm/RIU and Q factor attained is 257. The dimension of the biosensor is nano structure having size of $12\mu\text{m} \times 8\mu\text{m}$, it can be embedded in hand held devices.

Future Scope

Work can be carried for designing a sensor to detect COVID-19 by using the refractive index of infected person.

Limitation

Major limitation of this biosensor is accurate fabrication, error in dimension leads to faulty product and accurate coupling of light inside the waveguide.

6 Acknowledgement

HK thanks research guides, friends and lab technicians for guiding this work.

References

- 1) Liu R, Cai Z, Zhang Q, Yuan H, Zhang G, Yang D. Colorimetric two-dimensional photonic crystal biosensors for label-free detection of hydrogen peroxide. *Sensors and Actuators B: Chemical*. 2022;354:131236–131236. Available from: <https://dx.doi.org/10.1016/j.snb.2021.131236>.
- 2) Rashidnia A, Pakarzadeh H, Hatami M, Ayyanar N. Photonic crystal-based biosensor for detection of human red blood cells parasitized by plasmodium falciparum. *Optical and Quantum Electronics*. 2022;54:1–9. Available from: <https://dx.doi.org/10.1007/s11082-021-03421-w>.
- 3) Bijalwan A, Singh BK, Rastogi V. Analysis of one-dimensional photonic crystal based sensor for detection of blood plasma and cancer cells. *Optik*. 2021;226:165994–165994. Available from: <https://dx.doi.org/10.1016/j.ijleo.2020.165994>.
- 4) Dinodiya S, Bhargava A. Biosensor Based on One-Dimensional Photonic Crystal for Poliovirus Detection. In: *Lecture Notes in Mechanical Engineering*; vol. 2022. Springer Singapore. 2022;p. 303–310. Available from: https://doi.org/10.1007/978-981-16-5371-1_26.
- 5) Kundal S, Bhatnagar A, Sharma R. 1D Photonic Crystal Waveguide Based Biosensor for Skin Cancer Detection Application. In: *Lecture Notes in Electrical Engineering*. Springer Singapore. 2022;p. 443–450. Available from: https://doi.org/10.1007/978-981-16-2818-4_47.

- 6) Arishi WA, Alhadrami HA, Zourob M. Techniques for the Detection of Sickle Cell Disease: A Review. *Micromachines*. 2021;12(5):519–519. Available from: <https://dx.doi.org/10.3390/mi12050519>.
- 7) Wu N, Zhang HC, Sun XH, Guo FN, Feng LX, Yang T, et al. Detection of HIV/HCV virus DNA with homogeneous DNA machine-triggered in situ formation of silver nanoclusters. *Sensors and Actuators B: Chemical*. 2022;352:131041–131041. Available from: <https://dx.doi.org/10.1016/j.snb.2021.131041>.
- 8) Singh J, Singh R, Singh S, Mitra K, Mondal S, Vishwakarma S, et al. Colorimetric detection of hydrogen peroxide and cholesterol using Fe₃O₄-brominated graphene nanocomposite. *Analytical and Bioanalytical Chemistry*. 2022;414(6):2131–2145. Available from: <https://dx.doi.org/10.1007/s00216-021-03848-w>.
- 9) Aly AH, Mohamed D, Zaky ZA, Matar ZS, El-Gawaad NSA, Shalaby AS, et al. Novel Biosensor Detection of Tuberculosis Based on Photonic Band Gap Materials. *Materials Research*. 2021;24(3). Available from: <https://dx.doi.org/10.1590/1980-5373-mr-2020-0483>.
- 10) Miyan H, Agrahari R, Gowre SK, Mahto M, Jain PK. Computational Study of a Compact and High Sensitive Photonic Crystal for Cancer Cells Detection. *IEEE Sensors Journal*. 2022;22(4):3298–3305. Available from: <https://dx.doi.org/10.1109/jsen.2022.3141124>.
- 11) Khan MRH, Ali FAM, Islam MR. THz sensing of CoViD-19 disinfecting products using photonic crystal fiber. *Sensing and Bio-Sensing Research*. 2021;33:100447–100447. Available from: <https://dx.doi.org/10.1016/j.sbsr.2021.100447>.
- 12) Sani MH, Ghanbari A, Saghaei H. High-sensitivity biosensor for simultaneous detection of cancer and diabetes using photonic crystal microstructure. *Optical and Quantum Electronics*. 2022;54:1–4. Available from: <https://dx.doi.org/10.1007/s11082-021-03371-3>.
- 13) Panda A, Vigneswaran D, Pukhrambam PD, Ayyanar N, Nguyen TK. Design and Performance Analysis of Reconfigurable 1D Photonic Crystal Biosensor Employing Ge₂Sb₂Te₅ (GST) for Detection of Women Reproductive Hormones. *IEEE Transactions on NanoBioscience*. 2022;21(1):21–28. Available from: <https://dx.doi.org/10.1109/tnb.2021.3107592>.
- 14) Daher MG, Taya SA, Colak I, Vigneswaran D, Olaimat MM, Patel SK, et al. Design of a nano-sensor for cancer cell detection based on a ternary photonic crystal with high sensitivity and low detection limit. *Chinese Journal of Physics*. 2022;77:1168–1181. Available from: <https://dx.doi.org/10.1016/j.cjph.2022.03.032>.
- 15) Kundal S, Bhatnagar A, Sharma R. 1D Photonic Crystal Waveguide Based Biosensor for Skin Cancer Detection Application. In *Optical and Wireless Technologies 2022*. Singapore. Springer. . Available from: https://doi.org/10.1007/978-981-16-2818-4_47.
- 16) Mafi M, Esmail AH. Inverse design of a high-quality factor multi-purpose optical biosensor. *IET Optoelectronics*. 2022. Available from: <https://dx.doi.org/10.1049/ote2.12066>.
- 17) Nohoji AHA, Danaie M. Highly Sensitive Refractive Index Sensor based on Photonic Crystal Ring Resonators Nested in a Mach-Zehnder Interferometer. Available from: <https://doi.org/10.21203/rs.3.rs-1396678/v1>.